Measurement of the secular motion frequency and the space charge density in the linear ion trap*

Zhou Fei(周 飞)[a)b)], Xie Yi(谢 艺)[a)b)], Xu You-Yang(徐酉阳)[a)b)], Huang Xue-Ren(黄学人)[a)], and Feng Mang(冯 芒)[a)†]

[a)] *State Key Laboratory of Magnetic Resonance and Atomic and Molecular Physics, Wuhan Institute of Physics and Mathematics, Chinese Academy of Sciences, Wuhan* 430071, *China*

[b)] *Graduate School of the Chinese Academy of Sciences, Beijing* 100039, *China*

(Received 29 March 2010; revised manuscript received 28 April 2010)

This paper reports that a cloud of laser-cooled $^{40}Ca^{+}$ is successfully trapped and manipulated in the home-built linear ion trap constructed for quantum information processing (QIP). The frequency of the secular motion and the space charge density of the ion cloud are measured, which help knowing the characteristic of the trapping potential and are the prerequisite of QIP with the trapped ions.

Keywords: trapped ions, secular motion frequency, space charge
PACC: 3280P, 4250, 0367

1. Introduction

Over the past two decades, quantum information processing (QIP) has made great progress in both theory and experiment by combining physics, informatics and computer science.[1] There have been several candidate systems proposed as future quantum information processors, where the trapped ion system is one of the most promising candidates due to full controllability of the ionic qubits and long coherence time of the ionic states.[2] So far, some QIP implementations have been demonstrated with trapped ions[3−7] and entanglement of up to eight ions has been achieved.[8] Recent experiments have also shown the availability of quantum simulation with trapped-ion QIP[9] and the possibility of large-scale trapped-ion QIP.[10]

In this paper we study experimentally a large number of $^{40}Ca^{+}$ ions confined as a cloud and laser-cooled in our home-built linear Paul trap. The linear Paul trap was built solely for QIP study, such as entanglement generation, gate operation and quantum state transfer. It has been proposed that the cloud of laser-cooled ions in trap could work as a quantum memory[11] and be used to test some quantum phenomena.[2] Besides, considering the ion cloud as an ensemble of spins, one may carry out some interesting tasks of QIP on this ensemble qubit[13] To accomplish the above jobs, however, we have to first understand the characteristic of the trapping potential. To this end, we need to measure the frequency of the secular motion of the trapped ions and also investigate the space charge density in our trap. The frequency of the secular motion of the trapped ions is essential to the calculation of the geometrical factors of our linear trap. It also determines the Doppler cooling limit and the speed of quantum gating in the trap. Moreover, with the measured frequency of the secular motion, we could obtain the space charge density of the ions in our trap, which is relevant to the capacity and the structure of the trapping potential.

The paper is structured as follows. The next section presents the basic theory for the ion trapping and the space charge density of the trapped ions. Then we demonstrate our measured results of the secular motion frequency and the space charge density in our ion-trap system in Section 3. Brief discussion and conclusion are made in Section 4.

*Project supported by the National Natural Science Foundation of China (Grant Nos. 10774161, 10774163 and 10974225), and by National Fundamental Research Program of China (Grant No. 2006CB921203).
†Corresponding author. E-mail: mangfeng@wipm.ac.cn
© 2010 Chinese Physical Society and IOP Publishing Ltd

2. The theory of ion cloud trapping

2.1. The trapping potential

As shown in Fig. 1, the linear ion trap we built consists of four radio frequency (RF) blade-like electrodes and two DC tip-like electrodes. To reduce the stray DC field in the trap, we also have two compensation electrodes. If we define our Cartesian axes such that the z-axis is along the trap, the confinement potential produced by the RF electrodes is

$$\Phi_{\rm rf}(x,y,t) = \alpha_{\rm ac} V_{\rm rf} \frac{x^2-y^2}{r_0^2} \cos(\Omega_{\rm rf} t), \tag{1}$$

where $\alpha_{\rm ac}$ is the geometrical correction factor in the x–y plane perpendicular to the trap axis and $r_0 = 0.8$ mm is the distance from the trap axis to the nearest surface of the RF electrodes. The $\Omega_{\rm rf}$ is the trap driven frequency, which is produced by the RF source with amplitude of $V_{\rm rf}$. The axial confinement potential is generated by the tips (also called end-caps), which is defined as

$$\Phi_{\rm tip}(x,y,z) = \frac{\alpha_z U_{\rm tip}}{L^2}\left[z^2 - \frac{x^2+y^2}{2}\right], \tag{2}$$

where α_z is the geometrical correction factor along the z-axis, L is the distance between the trap centre and the DC tip, and $U_{\rm tip}$ is the voltage applied on the tips. As a result, the whole potential in the linear trap is

$$\Phi = \Phi_{\rm rf} + \Phi_{\rm tip}. \tag{3}$$

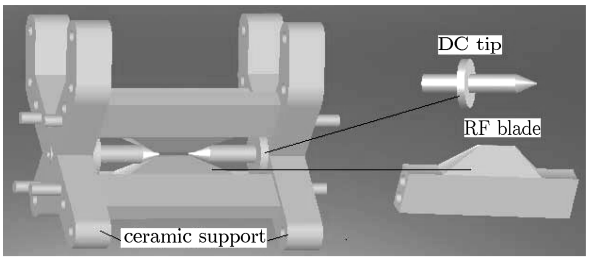


Fig. 1. Our home-built linear ion trap, where the distance between the axial (tip) electrodes is 5.0 mm and the distance between two diagonal radial (blade) electrodes is 1.6 mm. Two compensation electrodes are installed near two of the blades.

Consider a single calcium ion with the charge +e and the mass M trapped in above potential. The force on the ion is $F = -e\nabla\Phi$, which, with $\Omega_{\rm rf} t = 2\tau$, leads to the Mathieu equation,[14]

$$\mathrm{d}^2u/\mathrm{d}\tau^2 + [a - 2q\cos(2\tau)]u = 0, \tag{4}$$

where $u = u_x\hat{\boldsymbol{e}}_x + u_y\hat{\boldsymbol{e}}_y + u_z\hat{\boldsymbol{e}}_z$ is the position of the trapped ion with the stability parameters a and q defined as,

$$a = \frac{-e\alpha_z U_{\rm tip}}{ML^2\Omega_{\rm rf}^2}, \tag{5}$$

$$q = \frac{2e\alpha_{\rm ac} V_{\rm rf}}{Mr_0^2\Omega_{\rm rf}^2}. \tag{6}$$

The components of q in three dimensions are defined by $q_x = -q_y = q$ and $q_z = 0$. The components of a are given by $a_x = a_y = -a_z/2 = a$.

In case of $a, q \ll 1$, the first-order solution to Eq. (4) is given by

$$u_i(t) = u_0\cos(\omega_i t)\left[1 + \frac{q_i}{2}\cos(\Omega_{\rm rf} t)\right], \tag{7}$$

where $i = x, y, z$ and ω_i is the secular motion frequency in the three dimensions. For the radial directions, we have

$$\omega_x = \omega_y = \omega_r = \frac{\Omega_{\rm rf}}{2}\sqrt{a_i + \frac{q_i^2}{2}}, \tag{8}$$

and in the axial direction we have

$$\omega_z = \sqrt{\frac{e\alpha_z U_{\rm tip}}{2ML^2}}. \tag{9}$$

In the presence of external electric stray fields, the trapped ions would probably deviate from the original equilibrium positions, which increases the amplitude of the micromotion. This excess micromotion is one of the origins of heating in the ion trap, which could be suppressed by the compensation electrodes to which appropriate DC voltages are applied.

2.2. Space charge effect

It is important to understand the space charge effect in our trap potential after a large number of ions have been loaded.[15] The mean force on any of the trapped ions from the quadrupole field averaged over an RF cycle is

$$\begin{aligned}\bar{F}_q &= -M\omega_x^2\bar{u_x} - M\omega_y^2\bar{u_y} - M\omega_z^2\bar{u_z} \\ &= -\nabla\psi(\bar{u_x}, \bar{u_y}, \bar{u_z}),\end{aligned} \tag{10}$$

where $\bar{u_i}$ with $i = x, y, z$ is the average of the ion's position, and $\psi(\bar{u_x}, \bar{u_y}, \bar{u_z})$ is from the harmonic pseudopotential of the trap

$$\psi = \frac{1}{2}M\omega_x^2 u_x^2 + \frac{1}{2}M\omega_y^2 u_y^2 + \frac{1}{2}M\omega_z^2 u_z^2. \tag{11}$$

In addition to the force from the quadrupole field, the trapped ion also experiences the electrostatic repulsion from other ions. The averaged potential due to the ions is given by Poisson equation

$$\nabla^2\phi = -\frac{\rho}{\epsilon_0},$$

where ρ is the averaged ionic charge density and ϵ_0 is the permittivity of vacuum. In the case of zero temperature with no secular motion and no ion–ion collisions, the averaged force $\bar{F}_q$ acting on an ion from the quadrupole field should be counterbalanced by the repulsive force $\bar{F}_i$ due to the other ions. So we have $\bar{F}_i + \bar{F}_q = 0$, where $\bar{F}_i = -e\nabla\phi(\bar{u_x}, \bar{u_y}, \bar{u_z})$. Using Eq. (10) and the above Poisson equation, we could obtain the charge density

$$\rho = \frac{\epsilon_0 M}{e}(2\omega_r^2 + \omega_z^2). \tag{12}$$

In the case of zero temperature, the shape of the ion cloud is a perfect ellipsoid of constant density with the ellipticity changing with the locations in the pseudopotential. In the case beyond zero temperature, the motional energy of each ion should be equivalent in all three dimensions, which means the equipotential surface as the boundary of the ion cloud. We may define the ellipticity as

$$e = \frac{\omega_r}{\omega_z}. \tag{13}$$

3. Experimental measurement

3.1. Experimental setup

As shown in Fig. 2, our linear ion trap is encapsulated in a vacuum chamber connected to a 40 L/s ion pump (Varian) plus a titanium sublimation pump (Varian).

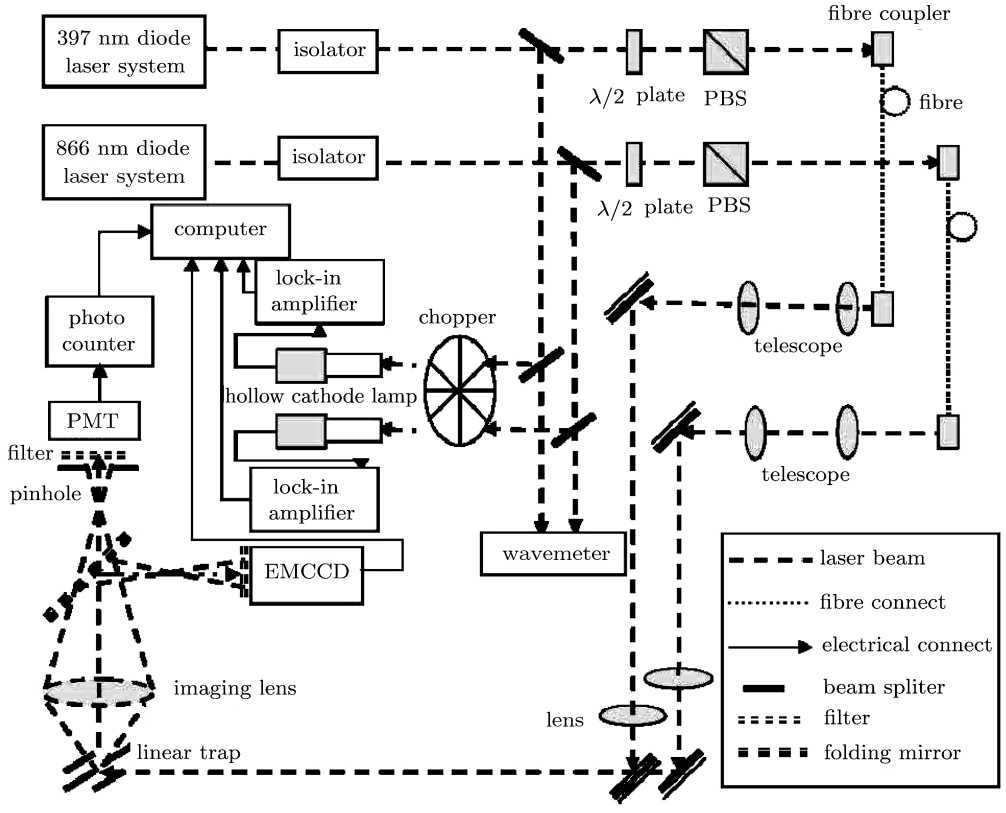


Fig. 2. Schematic drawing of our home-built linear ion trap system, where the details are explained in the text.

The pressure lower than 10^{-7} Pa in the chamber is indicated from the measurement of the ion current smaller than 0.1 μA by the ion pump. For trapping the ions, a home-made RF source at 19.6 MHz is applied to the blades with the tunable power from 0.5 W to 15 W. The ions are produced in the trap centre by the electron bombardment on an atomic beam from the calcium oven. After loading $^{40}Ca^+$ ions in the trap,

we cool them by two diode lasers with wavelengths 397 nm (DL100 Toptica) and 866 nm (home made). The two laser beams are overlapped and focused on the centre of the trap, where the power and the beam waist are 50 μW and 50 μm respectively for 397 nm laser, and 200 μW and 100 μm respectively for 866 nm laser. The laser scheme could be found in Fig. 3.

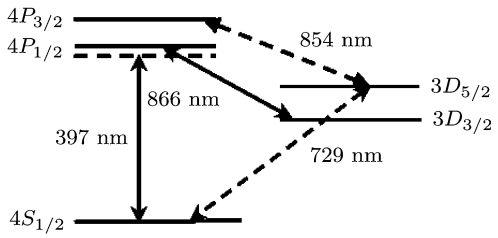


Fig. 3. Energy levels of $^{40}Ca^{+}$ employed for the ion trap QIP, where 729 nm and 854 nm lasers are not used in the present work, but will play important roles in sideband cooling and quantum gating.

The detection is made by both photon counting and imaging. The photon counting system consists of a set of microscope objective with an enlargement factor of 7, a photo multiplier tube (PMT) (9893QSB, EMI) plus a fast preamplifier (SR445A, Stanford research systems) and a photon counter (SR400, Stanford research systems). The fluorescence is collected by the microscope objective, and then focused onto a 1.2 mm-diametre pinhole in front of the PMT. The data are recorded by the PMT and finally stored by a computer system. The imaging system shares the same microscope objective with the PMT, and demonstrates the image of the ions by an electron-multiplying coupled-charge device (EMCCD) (PhotonMax: 512B, PI) camera. The successful trapping of the ions could be evidenced by both the PMT and the EMCCD camera.

3.2. Observation of the ion cloud

In order to study the property of the ion clouds, we have loaded hundreds of $^{40}Ca^{+}$ ions and radiated them by cooling lasers, where the 397 nm laser was scanned from 1 GHz red detuning to the near resonance and the 866 nm repumping laser was always at the resonance. Under appropriate trapping condition, the ions stay stably as a cloud, whose fluorescence collected by the EMCCD presents the image shown in Fig. 4.

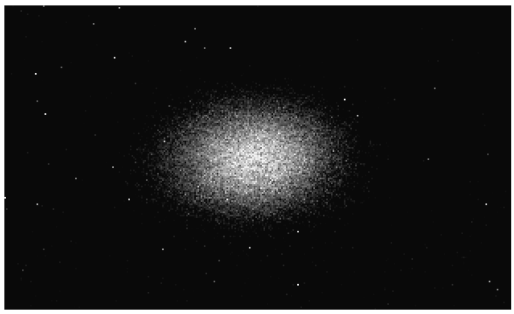


Fig. 4. The image of the ion cloud on the EMCCD.

We have changed the trapping potential in the trap by adjusting the voltages on the compensation electrodes, the blades and the tips. Since the ion cloud always moves toward the lowest energy point of the potential, we could fully control the position of the ion cloud in the trap.

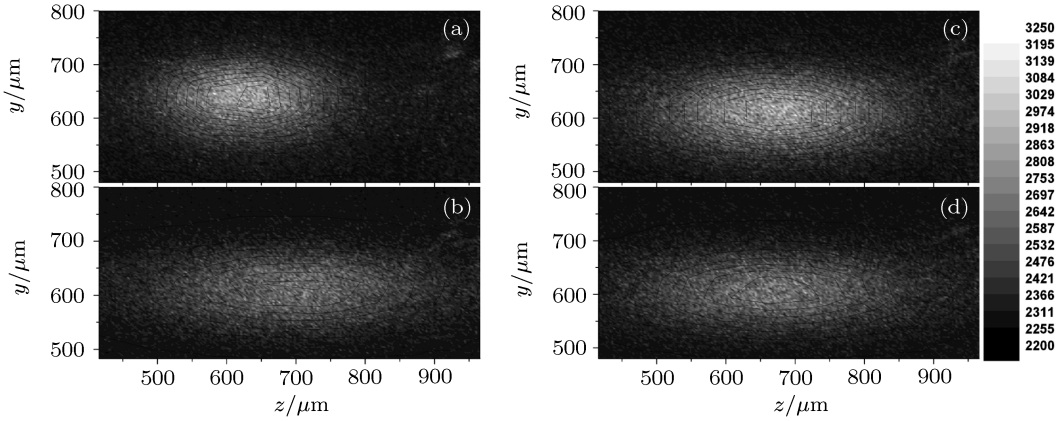


Fig. 5. The outputs of the two-dimensional Gaussian fitting corresponding to the ion cloud images, where (a) the RF power is 6 W and the tip voltage is 500 V; (b) the RF power is 6 W and the tip voltage is 50 V; (c) the RF power is 4 W and the tip voltage is 100 V; (d) the RF power is 10 W and the tip voltage is 100 V.

To fully confine the ions, however, we have to make sure that the ions stayed in the stability region. This means that the stability parameters a and q should satisfy $a \ll q < 1$. On the other hand, as the shape of the ion cloud depends on the balance between the trapping potential and the Coulomb repulsion, our adjustment of the external voltages could determine the size and the shape of the cloud. This is the prerequisite of QIP with the trapped ions. A series of images of such ion cloud were taken with the varied trapping parameters. Figure 5 is the two-dimensional Gaussian fitting for these images on the EMCCD, from which we could know accurately the sizes of the ion clouds.

Figures 6(a) and 6(b) present the ellipticities of the ion clouds varied with the trapping voltages. To understand the changes, we have made some calculations to fit the experimental values, where the good fittings imply the high-quality of the trapping potential in our setup. The small deviation is probably due to the thermal fluctuation of the ions' motion and the inhomogeneous potential caused by the deposit of the material patches from the oven beam on the electrodes. To eliminate these imperfection, we will further cool the ions to the Doppler cooling limit and clean the trap as much as we can.

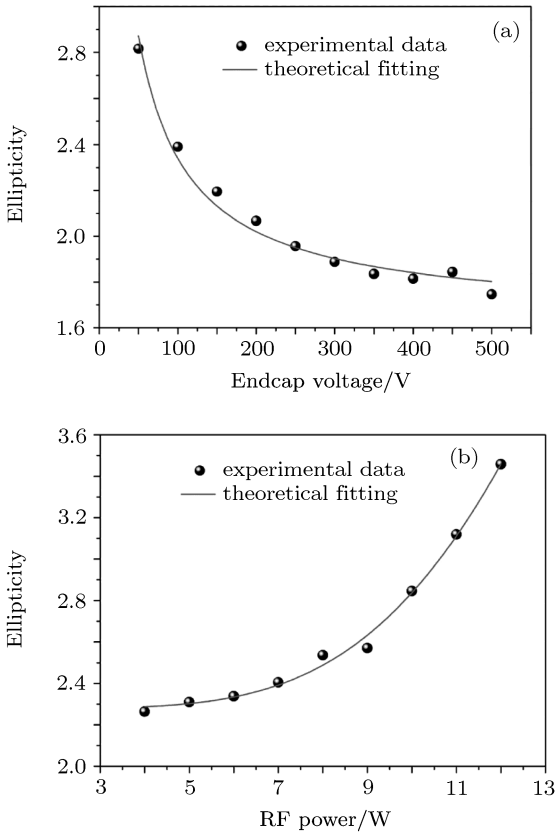


Fig. 6. The changes of the ellipticities with respect to the trapping voltages on (a) the tips and (b) the blades.

Alternatively, we will replace the electron bombardment by photoionization in the future for more efficiently producing the calcium ions, which would largely reduce the deposit of the patches on the electrodes.

3.3. Measurement of the secular motion frequency and space charge effect

Since our trap works well and the trapped ions are fully under our control, we could measure the secular motion frequency of the ions by the RF field resonance method.[16,17] After loading the ions, we carefully adjusted the compensation voltages to push the ions to the potential centre where the excess micromotion is minimum and the Doppler cooling works more efficiently. Then we applied a weak RF voltage to a tip electrode or a compensation electrode for driving the ions' motion. By scanning the frequency of the driving RF field (produced by Agilent 33220A), we have observed the signal of the resonant fluorescence, which implies the resonance between the weak RF driving and the secular motion of the ions. The ions were heated up at the resonance and thereby a drop in the fluorescence spectrum was observed, this is demonstrated as an example in Fig 7 for ω_z.

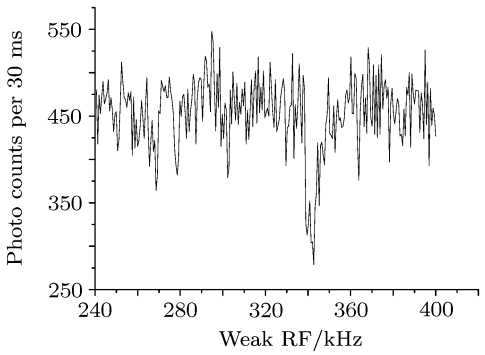


Fig. 7. The measurement of the secular motion frequency ω_z of the trapped ions by a small RF voltage ($V_{\mathrm{p-p}} = 5$ V) applied to a tip electrode. The drop in the spectrum means the resonance between the RF driving and the axial secular motion of the trapped ions.

Using the measured values of the secular motion frequencies ω_r and ω_z, we may obtain the stability parameters and the geometric correction factors. Some of our results are listed in Tables 1 and 2. Since the geometric correction factors are almost constant, the values obtained here will be employed in our future experiments for QIP.

Table 1. Axial secular motion frequencies, values of a and the corresponding voltages $U_{\rm tip}$, where the RF power is 3 W and the horizontal compensation voltage is −62 V. From the data, we know the geometric correction factor $\alpha_z = 0.1454$.

$U_{\rm tip}$/V	$(\omega_z/2\pi)$/kHz	a
60	420	0.0009
70	445	0.0010
80	470	0.0012

Table 2. Radial secular motion frequencies and values of q with corresponding RF power, where the tip voltage is 30 V and the horizontal compensation voltage is −73 V. From the data, we know the geometric correction factor $\alpha_{\rm ac} = 0.1898$.

RF power/W	$(\omega_r/2\pi)$/kHz	q
2	750	0.1122
3	980	0.1445
4	1130	0.1657
5	1360	0.1984

In order to calculate the value of q and $\alpha_{\rm ac}$, we have to measure the accurate value of the rf voltage applied to the trap. As shown in Fig. 8, the RF voltage is generated by a signal generator (Rohde & Schwarz 1000 kHz. SMX) followed by an amplifier (Mini-Circuits LZY-1). The power of the helical resonator as well as the reflected power are measured by a power meter (Diamond SX-200). The helical resonator is installed between the power meter and the RF electrodes, which is used for further RF amplification and for impedance matching of the open-ended circuit. To measure the RF voltage on the RF electrodes, we applied the RF signal to the capacitance divider and read the voltage values on the oscilloscope. As shown in Fig. 9, we have measured the high voltage up to 2000 V, and also fitted the experimental data by a theoretical formula. The imperfection in the fitting comes from the power loss in the RF transmission.

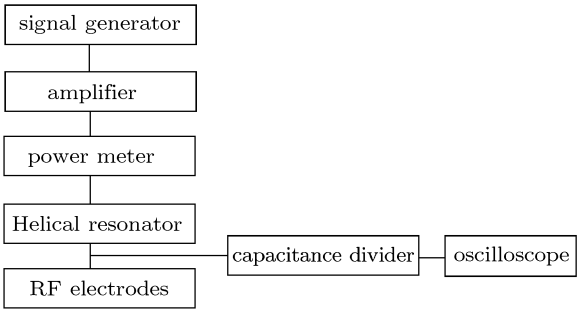


Fig. 8. Functional block diagram of the RF source and the RF voltage measurement scheme .

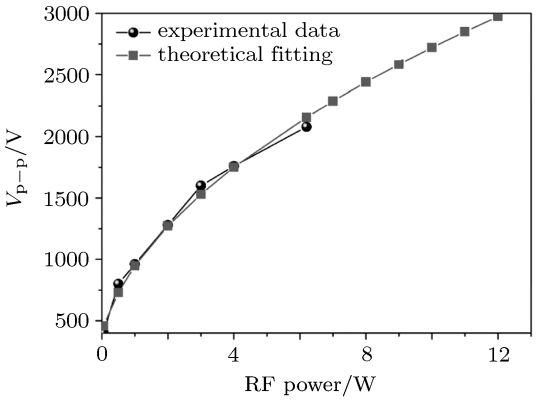


Fig. 9. The RF voltage changed with the input power, where the theoretical fitting for the voltage larger than 2000 V is made by our deduced formula $V_{\rm p-p} = \sqrt{7.228 \times 10^5 P + 1.741 \times 10^5}$ with P the input power.

Based on the above measurements, we have analysed in Table 3 the space charge density and the ion number in Fig. 5, using the equations in Subsection 2.1. For each loading, the numbers of the trapped ions are fixed. We may enlarge or decrease the ion density by changing the trapping potential.

Table 3. The charge density of the ion cloud and the number of ions changed with different trapping potentials, where the first and second rows belong to a different loading from the third and fourth rows.

$U_{\rm tip}$/V	P/W	$(\rho/e)/(10^{15}$ ion/m$^3)$	N
50	6	2.1645	407
500	6	9.1133	407
100	4	2.8873	444
100	10	4.416	444

4. Discussion and conclusion

Since the ion trap could provide a clean and nearly isolate space for confinement, the trapped ions are good qubit carriers for QIP. There are more than 25 groups worldwide working with trapped ion for QIP, where the most leading groups are in NIST, USA for ^{9}Be$^+$[3] and in Innsbruck, Austria for ^{40}Ca$^+$.[5] Besides, some other groups are exploring other candidate ions, such as ^{111}Cd$^+$,[18], ^{171}Yb$^+$,[19,20] ^{43}Ca$^+$,[6] ^{138}Ba$^+$[21] and ^{88}Sr$^+$.[22] Moreover, the scalable QIP with the trapped ions could be hopefully carried out by moving the ions from one zone to another in a multi-trap device[23] or by entangling spatially separated ions using photonic emission.[7] Since these works are based on linear ion traps, it is believed that the individual linear ion trap is the basic component and includes the key technique for future large-scale ion trap QIP.

To have the ions doing more QIP tasks, we will further cool the ions by sideband cooling technique down to the vibrational ground state. Due to the Coulomb repulsion and the RF heating, the trapped ions collide strongly with each other in the trap. So only when the cooling rate is much larger than the heating rate, will the ion cloud turn to the ion crystallization, which will allow us to encode and manipulate qubits individually in separated trapped ions for accomplishing some interesting QIP tasks.[24−26]

In summary, a cloud of laser-cooled $^{40}Ca^{+}$ ions have been loaded and manipulated in our home-built linear trap, which could be employed as an ensemble to store quantum information and to accomplish quantum gating. We have tried to optimise the trapping condition using external voltages, based on which we have measured the secular motion frequency of the trapped ions and studied the space charge density in our trap. These are the prerequisites for carrying out QIP with our setup. As the ion cloud is well controlled, we are confident that the QIP implementation will soon be on the way.

Acknowledgement

We acknowledge thankfully for Guan Hua, Guo Bin, Chen Liang and Liu Qu for discussion and help, and we are grateful to Prof. Zhan Mingsheng and Prof. Gao Kelin for their support and encouragement.

References

[1] Ladd T D, Jelezko F, Laflamme R, Nakamura Y, Monroe C and O'Brien J L 2010 *Nature* **464** 45
[2] Blatt R and Wineland D J 2008 *Nature* **453** 1008
[3] Monroe C, Meekhof D M, King B E, Itano W M and Winland D J 1995 *Phys. Rev. Lett.* **75** 4714
[4] Gulde S, Riebe M, Lancaster G P T, Becher C, Eschner J, Häffner H, Schmidt-Kaler F, Chuang I L and Blatt R 2003 *Nature* **421** 48
[5] Riebe M, Häffner H, Roos C F, Hänsel W, Benhelm J, Lancaster G P T, Körber T W, Becher C, Schmidt-Kaler F, James D V F and Blatt R 2004 *Nature* **429** 734
[6] Roos C F, Chwalla M, Kim K, Riebe M and Blatt R 2006 *Nature* **443** 316
[7] Moehring D L, Maunz P, Olmschenk S, Younge K C, Matsukevich D N, Duan L M and Monroe C 2007 *Nature* **449** 68
[8] Häffner H, Hänsel W, Roos C F, Benhelm J, Chek-al-kar D, Chwalla M, Körber T, Rapol U D, Riebe M, Schmidt P O, Becher C, Gühne O, Dür W and Blatt R 2005 *Nature* **438** 643
[9] Gerritsma R, Kirchmair G, Zähringer F, Solano E, Blatt R and Roos C F 2010 *Nature* **463** 68
[10] Home J P, Hanneke D, Jost J D, Amini J M, Leibfried D and Wineland D J 2009 *Science* **325** 1227
[11] Coudreau T, Grosshans F, Guibal S and Guidoni L 2007 *J. Phys.* B **40** 413
[12] Herskind P, Dantan A, Langkilde-Lauesen M B, Mortensen A, Sørensen J L and Drewsen M 2008 *Appl. Phys.* B **93** 373
[13] Biercuk M J, Uys H, VanDevender A P, Shiga N, Itano W M and Bollinger J J 2009 *Nature* **458** 996
[14] Paul W 1990 *Rev. Mod. Phys.* **62** 531
[15] Ghosh P K 1995 *Ion Trap* (New York: Oxford University Press) p23
[16] Wineland D J and Dehmelt H 1975 *Int. J. Mass Spectrum. Ion Phys.* **16** 338
[17] Guo B, Guan H, Liu Q, Huang Y, Huang X R and Gao K L 2010 *Chin. Phys. Lett.* **27** 013202
[18] Blinov B B, Moehring D L, Duan L M and Monroe C 2004 *Nature* **428** 153
[19] Olmschenk S, Younge K C, Moehring D L, Matsukevich D N, Maunz P and Monroe C 2007 *Phys. Rev.* A **76** 052314
[20] Wunderlich C, Balzer C, Hannemann T, Mintert F, Neuhauser W, Reiß D and Toschek P E 2003 *J. Phys.* B **36** 1063
[21] Kurz N, Dietrich M R, Shu G, Bowler R, Salacka J, Mirgon V and Blinov B B 2008 *Phys. Rev.* A **77** 060501
[22] Wang S X, Labaziewicz J, Ge Y, Shewmon R and Chuang I L 2009 *Appl. Phys. Lett.* **94** 094103
[23] Leibfried D, DeMarco B, Meyer V, Rowe M, Ben-Kish A, Barrett M, Britton J, Hughes J, Itano W M, Jelenkovic B M, Langer C, Lucas D, Rosenband T and Wineland D J 2003 *J. Phys.* B **36** 599
[24] Feng M, Hai W H, Zhu X W, Gao K L and Shi L 2000 *Chin. Phys.* **9** 250
[25] Zheng X J, Fang M F, Cai J W and Liao X P 2006 *Chin. Phys.* **15** 492
[26] Zheng X J, Luo Y M and Cai J W 2009 *Chin. Phys.* **18** 1352